

Mass flow rate and tangential momentum accommodation coefficient from experiments in a single micro tube

Timothée Ewart, Pierre Perrier, Irina A. Graur and J. Gilbert Méolans

*Université de Provence - Ecole Polytechnique Universitaire de Marseille, Département de Mécanique
Energétique - UMR CNRS 6595, 5 rue Enrico Fermi, 13453 Marseille cedex 13, France*

Abstract. Experimental investigations of isothermal steady flows for various gases have been carried out in a silica micro tube. The study is focused on the mass flow rate measurements of these flows in slip regime, using a suitable powerful platform. First we analyse, for each gas, the pertinence of a first or second order continuum treatment; then we deduce from experiments, using the appropriate treatment, the tangential momentum accommodation coefficient (TMAC) of each gas. The TMAC obtained for the various pairs of gas (nitrogen, argon, helium)/surface (fused silica) exclude a full diffuse reflection.

Keywords: Tangential momentum accommodation, microscale flows, mass transfer, micro fluidics, pressure measurements, wall interactions
PACS: 47.61.Fg

INTRODUCTION

The Micro-Electro-Mechanical-Systems open a new area in the rarefied gas experiments. Indeed, since the early eighties and the beginning of the MEMS, a lot of micro devices were designed to study gas micro flows. But channel geometries involving a rectangular (or trapezoidal) cross section have been privileged until to now [1] - [7]. In this work we present a gas micro flow study based on micro tube experiments. In this geometry the experiments are rare, only four different experiments involving rarefied gas flows in tubes or micro tubes have been undertaken in the last fifty years: using a tube with 3.64 cm of diameter in [8]; with a package of 10 tubes of a mean radius equal to 199.7 μm and also in a package of 100 tubes of a mean radius equal to 50 μm in [9]; then in [10], where the author did not measure directly the diameter of the tubes and finally with a package of 50 tubes with a radius of 25 μm in [11]. Thus, nobody performed experiments in a single micro tube characterized by a diameter precisely known. One of the reasons of this lack is due to the difficulty of measuring mass flow rates so weak as those flowing in a single micro tube (smaller than 10^{-10} kg/s): in point of fact, in a tube the mass flow rate can be from 3 to 100 times lower than that found in a rectangular channel for the same inlet/outlet pressure ratio, with the same streamwise length, and with the same small critic geometric dimension, *i.e.* for the same values of the Knudsen number. Indeed, in micro tube the small dimension is necessary the diameter, involved in the cross sections by its square power, while in micro channel only one dimension of the rectangular section is necessary small: thus using a large width, *i.e.* a small height-to-width ratio it is possible to increase largely the flow rate without changing the Knudsen number. Let us add that, for same basic geometric reasons, the dynamics of the flow in the tubes is in any case a two-dimensional problem, contrarily to that occurs in the rectangular channels where the problem becomes three-dimensional when the height-to-width ratio is not small enough. Thus some experiments exist concerning the TMAC in MEMS but, according to our previous remarks, they occurred in rectangular channel geometries [4], [6] and [7] or using several tubes in a package [9]. In anyway these experiments remain very few numerous compared to those carried out in the molecular beam domain [12] which in many cases did not concern really the same coefficient. Therefore the present determination appears of some scientific interest.

In the present study, we measure low mass flow rates in a micro tube in a (0.003 – 0.3) Knudsen number range, corresponding to a slip regime. We obtain satisfactory measurements with Nitrogen, Argon, and Helium, notably implementing new powerful pressure sensors. Then we have tested, for each gas, the pertinence of a first and/or second order treatment, according to the Knudsen number, to describe our experimental results. Then using a general formulation of the slip velocity, written at the suitable order, the Navier-Stokes equations yield an analytical expression of the mass flow rate. Thus, comparing to the experimental curves, we deduce first the slip coefficient. Assuming then the usual Maxwell expression of the slip coefficient we deduce the TMAC for each gas. Finally the influence of various physical parameters on the TMAC is briefly discussed.

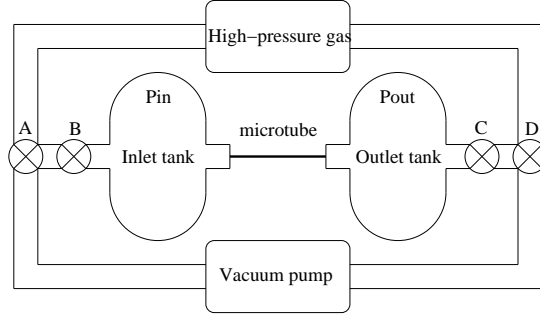


FIGURE 1. Schematic of experiment.

EXPERIMENTS

The experimental method used in the present work in order to measure the mass flow rate through a micro tube involves the use of two constant volume tanks and so may be denoted "constant-volume technique". This method requires very large tank volumes, much larger than the volume of the micro tube. Large tank sizes guarantee micro flow parameters independent of the time: although detectable (through their effects), the mass variations occurring in the tanks during the experiments should not call into question the stationary assumption. Thus, we have to fix a range for the maximal suitable pressure variations in the second tank, according to the inlet and outlet conditions. The experimental set up shown in Fig. 1 takes into account these constraints. The gas flows through a micro tube fixed between two tanks in which the pressures remain very close to constant values P_{in} and P_{out} , respectively. The maximum pressure variation in the second tank due to the gas flow through the micro tube is fixed at $\pm 1\%$ of the tank pressure averaged over the duration of the experiment. This variation range means that the required experiment duration τ will vary from 5 minutes for the highest mass flow rate measured (10^{-9} kg/s) to about 90 minutes for the lowest (10^{-13} kg/s).

Experiments were performed with a fused silica cylindrical micro tube. It is of great importance to measure the diameters of the tubes with a good accuracy because the analytical expression of the mass flow rate is proportional to the power four of the diameter. The surfaces of the inlet and outlet sections have been scanned in environmental scanning mode (ESEM) with an electron microscope, and the following estimation of the diameter is obtained: $D = 25.2 \pm 0.35 \mu\text{m}$. The roughness is estimated smaller than 0.1% of the diameter D . The diameter evaluation is also carried out indirectly, derived from the measured mass flow rate of Ar in the continuum flow regime ($Kn_m = 2.32 \times 10^{-3}$) which yields $D = 25.27 \pm 0.25 \mu\text{m}$. Moreover, the measure of the length of the tube gives $L_{tube} = 5.30 \pm 0.01 \text{ cm}$, which is much greater than the diameter, so the entrance and exit effects have been neglected.

Here, we omit the detailed description of methodology and experimental set-up. The validity of the measurements and modus operandi were approved in [13]. We will give here only the brief description of the measurement technique. Let us write for the second tank the equation of state for an ideal gas under the form:

$$P_{out}V = m\mathcal{R}T, \quad (1)$$

where V , \mathcal{R} , P_{out} , T and m are, respectively, the volume, the specific gas constant, the pressure, the temperature and the mass of the gas in the outlet tank at any time t of the experiment time length τ . Let us define the variation dq of any thermodynamic parameter q , occurring in the tank during the experiment time length. According to the previous comments, these relative variations remain small, compared to 1. Therefore, one obtains from (1):

$$\frac{dm}{\tau} = \frac{V}{\mathcal{R}T} \frac{dP_{out}}{\tau} (1 - \varepsilon), \quad \varepsilon = \frac{dT/T}{dP_{out}/P_{out}}. \quad (2)$$

In order to estimate ε we calculate firstly the temperature variation dT . In fact, when this variation is calculated directly from the standard deviation of the temperature recorded during the experiments [13], the value of dT is overestimated by the superposition of various noises (electronic and thermal noises) to the real thermal variations occurring in the tank. Therefore, two additional statistical processes are carried out in order to eliminate the influence of these noises on the temperature variation. Taking into account these estimations of the temperature variation and the pressure rise dP_{out} (fixed at $\pm 1\%$) we can conclude that $\varepsilon < 2 \cdot 10^{-2}$. Since ε is very small compared to 1, dm/τ

may be identified to the mass flow rate Q_m flowing from the micro tube, and dP_{out} allows direct measurement of Q_m :

$$Q_m = \frac{V}{\mathcal{R}T} \frac{\delta P_{out}}{\tau}. \quad (3)$$

The pressure measurements were carried out using simultaneously two detectors chosen according to the pressure range used in each experiment. In order to measure small pressure variations ($\delta P_{out} < 1\%$) high resolution detectors are used (from $2 \cdot 10^{-2} \text{ Pa}$ to 2 Pa). The errors in pressure measurements in each tank depend on the characteristics of the pressure detectors. In the pressure range observed during the experiments, the errors on the measurement of the outlet pressures were estimated smaller than 0.5%.

To determine the mass flow rate we will use the registered data for the pressure at the different time instants. The flow stationary conditions physically justify the pressure rise interpolation by means of a linear fitting function of time.

The usual evaluation of the measurements errors is applied and gives the following results: a full uncertainty on $\Delta Q_m/Q_m$ smaller than $\pm 4.5\%$, where the non-isothermal effects are previously evaluated as $\pm 2\%$; the uncertainty on the volume measure is $\pm 2\%$ and the error on coefficient of the linear fitting of the pressure measurements gives $\pm 0.5\%$. Moreover, the leaks were estimated with two different tests as totally negligible [13].

Finally it is to note that the capacities of the pressure sensors employed until now, have not allowed to reach the full developed transitional regime. We have determined a maximal measurement duration equal to 90 min to be in agreement with an ambient temperature remaining quasi constant. The smallest mass flow rate which we can measure in this time period with available sensors is equal to $6.38 \cdot 10^{-13} \text{ kg/s}$ and corresponds to Argon flow with $Kn_m = 0.219$. The corresponding values of the maximal Knudsen number for Nitrogen and Helium are equal to 0.247 and 3.0 respectively.

BACKGROUND THEORY

For many years, pressure-driven slip flows within ducts or channels have received considerable attention. Many formulations of analytical and semi-analytical solutions have been presented [14]. The analytical models derived from the Navier-Stokes equations or from other continuum equation systems require the use of the velocity slip boundary conditions. Several authors [6], [7] have recently proposed to use in this framework the velocity slip conditions of second-order according to the Knudsen number to take better into account the rarefied effects for the moderately rarefied gas flows.

In the hydrodynamic and slip regimes the flow through the micro tube have been intensively studied theoretically. Nevertheless the questions of the choice of appropriate boundary conditions (first or second order following the Knudsen number) and the question of the limit of validity of the continuum approach (in terms of the Knudsen number range) remains open question which are discussed below.

The flow analysis may be carried out with the Navier-Stokes equations with slip boundary conditions. Assuming a second order boundary condition at the wall the slip velocity reads:

$$u_s = \pm A_1 \lambda \left(\frac{\partial u}{\partial r} \right)_w - A_2 \lambda^2 \left(\frac{1}{r} \left(\frac{\partial}{\partial r} r \frac{\partial u}{\partial r} \right) \right)_w, \quad (4)$$

where λ is the mean free path of the molecules which could be calculated using the hard sphere (HS) model [15] where $k_\lambda = \sqrt{\pi}/2$, nevertheless, in this paper we used the variable hard sphere model (VHS) [16] more general than HS model. According to this model, coefficient k_λ is equal to $\frac{(7-2\omega)(5-2\omega)}{15\sqrt{\pi}}$, where ω , the viscosity index, depends on the type of gas:

$$\lambda = k_\lambda \frac{\mu}{P} \sqrt{2\mathcal{R}T}. \quad (5)$$

The coefficients A_1 and A_2 in (4) may be presented in the form:

$$A_1 = \frac{\sigma_p}{k_\lambda}, \quad A_2 = \frac{\sigma_{2p}}{k_\lambda^2}, \quad (6)$$

where σ_p and σ_{2p} are the first and second velocity slip coefficients that are assumed independent of the interaction model used in the gas.

The mass flow rate through the tube of diameter D , obtained from Navier-Stokes equations with the second order velocity slip condition [17], reads

$$\dot{M} = \frac{\pi D^4 \Delta P P_m}{128 \mu \mathcal{R} T L} \left(1 + 8A_1 Kn_m + 32A_2 \frac{P_m}{\Delta P} \ln \mathcal{P} Kn_m^2 \right), \quad (7)$$

where $\Delta P = P_{in} - P_{out}$, $\mathcal{P} = P_{in}/P_{out}$, Kn_m is the mean Knudsen number, based on the mean pressure $P_m = 0.5(P_{in} + P_{out})$. Furthermore, a non-dimensional mass flow rate S may be deduced from relation (7):

$$S = \dot{M} / \frac{\pi D^4 \Delta P P_m}{128 \mu \mathcal{R} T L} = 1 + 8A_1 Kn_m + 16A_2 \frac{\mathcal{P} + 1}{\mathcal{P} - 1} \ln \mathcal{P} Kn_m^2. \quad (8)$$

Expression (8) may be rewritten in the more compact form:

$$S = 1 + A^{theor} Kn_m + B^{theor} Kn_m^2. \quad (9)$$

The analytical expressions of the mass flow rate (7)-(9) will be used for the calculation and the comparison with the appropriate measured values. We will use the measured values of the mass flow rate to obtain the slip velocity coefficients and the "experimental" TMAC.

RESULTS AND DISCUSSION

We have studied the flows of Argon, Nitrogen and Helium in slip regime where the mean Knudsen number varies from 0.02 to 0.3. Each experiment was carried out with different pressure ratios $\mathcal{P} = [3, 4, 5]$ between the tanks, excepted N_2 which are limited to $\mathcal{P} = [3, 5]$. Figure 2 shows the experimental dimensionless mass flow rates (calculated according to (8)) for all the gases as a function of the mean Knudsen number.

In order to estimate the velocity slip coefficients the measured dimensionless mass flow rate was fitted with the first and second order polynomial form of the mean Knudsen number

$$S_f^{exp} = 1 + A_i^{exp} Kn_m + B_i^{exp} Kn_m^2, \quad i = 1, 2 \quad (10)$$

as it was detailed in [7] using a non-linear least square Marquard-Levenberg algorithm. Experimental fitting coefficients A_i^{exp} and B_i^{exp} , where $i = 1, 2$ and $B_1^{exp} = 0$, are calculated for all the gases and the uncertainty on these coefficients is calculated using the asymptotic standard error. These coefficients obtained for the pressure ratio $\mathcal{P} = 5$ are reported in Table 1. In order to analyze the respective pertinence of the first or the second order fitting for each gas two additional parameters are calculated: the determination coefficient r^2 and the residual variance $s_r = \sqrt{\frac{1}{n-p} \sum e_i^2}$, where $e_i = S_i^{exp} - S_{f_i}^{exp}$ is the local difference between the measured and fitting values, and so represents the local fitting error; n is the number of points and p is the number of unknown coefficients of the fitting model. Analyzing the values of these two coefficients, given in Table 1 only for $\mathcal{P} = 5$, (but the other \mathcal{P} values give similar results for these coefficients) we find that the determination coefficients r^2 of Argon and Nitrogen are essentially more close to 1 for the second order fitting. For the Helium flow the second order coefficients r^2 is also more close to 1 than the first order one, even if the difference between the two orders is here less important. Moreover, the values of the squared residual sum are also smaller for the second order fitting in the case of all the gases. In order to supplement this analysis, the residuals e_i (fitting errors) are plotted as a function of the averaged Knudsen number for the three gases. As an example, the residuals of Argon are presented in Fig. 2. The analysis of the form of the residuals distribution shows that the residuals of second order fit are equi-distributed, whereas the residuals of the first order fit are largely negative from 0.003 to 0.2 on the Knudsen axis, which confirms the choice of the second order fitting as more pertinent for Argon flows. The same analysis of the the form of residuals is carried out for Nitrogen and Helium. From this analysis we may conclude that the second order fitting appears clearly as the most pertinent for Nitrogen and Argon flows and also for the Helium flow: even if as shown in Table 1 the relative weight of the second order coefficient is smaller for Helium as for the other gases. Thus, in the sequel of this paper, we will use the results of the second order fitting for all the gases.

From the comparison of the theoretical and experimental non-dimensional mass flow rate expressions (9), (10) the coefficients A_1 and A_2 from the velocity slip boundary condition (4) and respectively the slip coefficients σ_p and σ_{2p}

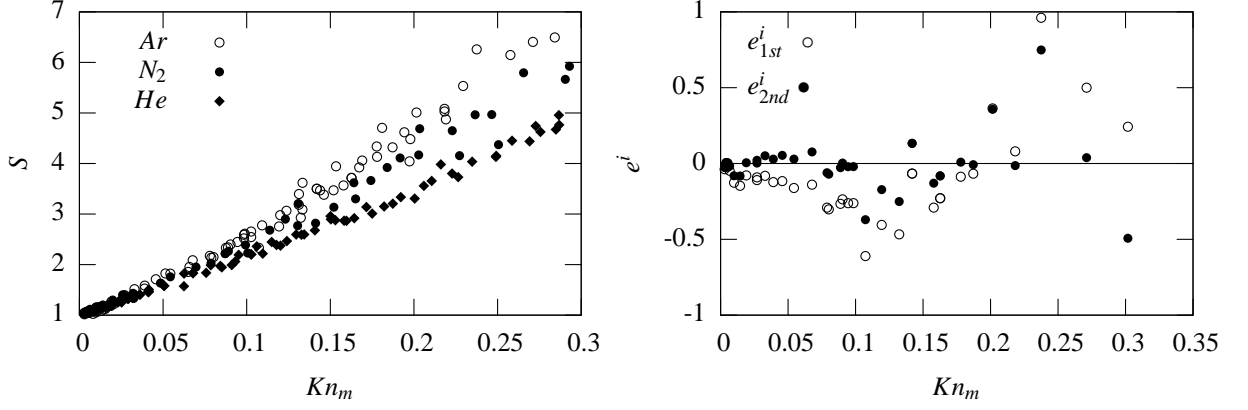


FIGURE 2. Dimensionless mass flow rate for N_2 , Ar and He gases obtained according to (8) and the Ar residuals for $\mathcal{P}_{Th} = 5$.

TABLE 1. Fitting parameters and TMAC obtained from present experiments ($\mathcal{P}_{Th} = 5$) and by other authors.

	Nitrogen	Argon	Helium		Nitrogen	Argon	Helium
A_{1st}^{exp}	15.49 ± 0.31	18.09 ± 0.37	12.99 ± 0.15	α_{1st}^{exp}	0.77 ± 0.01	0.71 ± 0.01	0.82 ± 0.01
A_{2nd}^{exp}	11.67 ± 0.97	13.27 ± 0.75	10.81 ± 0.37	α_{2nd}^{exp}	0.91 ± 0.04	0.88 ± 0.03	0.91 ± 0.02
B_{2nd}^{exp}	16.63 ± 4.06	24.05 ± 3.55	9.16 ± 1.50	[9]	0.925 ± 0.014	0.927 ± 0.028	0.895 ± 0.004
s_{r1st}	0.2115	0.2851	0.1315	[4]	$0.81 - 0.96$	$0.7 - 1$	-
r_{r1st}^2	0.9779	0.9691	0.9905	[7]	0.87 ± 0.03	-	0.91 ± 0.03
s_{r2nd}	0.1931	0.1903	0.0876	[6]	0.93	-	0.93
r_{r2nd}^2	0.9859	0.9863	0.9959				

may be found from the expressions:

$$A_1 = \frac{\sigma_p}{k_\lambda} = A^{exp}/8, \quad B^{exp} = 16A_2 \frac{\mathcal{P} + 1}{\mathcal{P} - 1} \ln \mathcal{P}, \quad A_2 = \frac{\sigma_{2p}}{k_\lambda^2}. \quad (11)$$

TABLE 2. σ_p^i and σ_{2p}^i experimental coefficients obtained from a polynomial fitting of first or second degree.

\mathcal{P}_{Th}	σ_p^{1st}	α^{1st}	σ_p^{2nd}	α^{2nd}	σ_{2p}^{2nd}	Kn_m
Nitrogen						
5	1.415 ± 0.028	0.770 ± 0.010	1.066 ± 0.009	0.908 ± 0.004	0.231 ± 0.057	0.003-0.291
3	1.464 ± 0.023	0.754 ± 0.008	1.242 ± 0.080	0.833 ± 0.031	0.253 ± 0.029	0.006-0.247
5 - 3	1.432 ± 0.019	0.765 ± 0.007	1.186 ± 0.062	0.856 ± 0.026	0.183 ± 0.045	0.003-0.291
Argon						
5	1.554 ± 0.034	0.726 ± 0.010	1.130 ± 0.068	0.879 ± 0.029	0.294 ± 0.045	0.003-0.302
4	1.564 ± 0.023	0.723 ± 0.008	1.169 ± 0.044	0.862 ± 0.018	0.290 ± 0.031	0.003-0.284
3	1.489 ± 0.029	0.746 ± 0.009	1.324 ± 0.106	0.802 ± 0.036	0.161 ± 0.010	0.003-0.219
5 - 3	1.544 ± 0.017	0.729 ± 0.005	1.176 ± 0.065	0.859 ± 0.024	0.283 ± 0.028	0.003-0.302
Helium						
5	1.277 ± 0.014	0.819 ± 0.005	1.062 ± 0.036	0.910 ± 0.017	0.147 ± 0.024	0.009-0.309
4	1.193 ± 0.036	0.852 ± 0.014	1.066 ± 0.015	0.908 ± 0.008	0.118 ± 0.011	0.011-0.300
3	1.260 ± 0.018	0.826 ± 0.007	1.044 ± 0.040	0.918 ± 0.018	0.166 ± 0.030	0.010-0.309
5 - 3	1.252 ± 0.009	0.829 ± 0.004	1.052 ± 0.020	0.914 ± 0.009	0.148 ± 0.014	0.009-0.309

The values of these coefficients are given in Table 2. We also derived an experimental value of the accommodation coefficient using the Maxwell diffuse-specular scattering model. The use of Maxwell's kernel for the gas-surface

interaction gives the following value for the velocity slip coefficient, neglecting the Knudsen layer influence:

$$\sigma_p^M = \frac{\sqrt{\pi}}{2} \frac{2 - \alpha}{\alpha}, \quad (12)$$

As well known, in the Maxwell kernel the same coefficient α may represent the energy accommodation as well as that of any momentum component. However, in isothermal slip regime it is usual and physically justified to identify α as the TMAC. In the case of a full accommodation ($\alpha = 1$) the theoretical coefficient σ_p^M is equal to 0.886. The different values of α are given in Table 2.

The previous data may be summarized as follows:

- in the investigated Knudsen range the relative weight of the second order effect (B_{2nd}/A_{2nd}) increases with the molecular mass and does not depend on the molecular internal structure (see Table 1).
- the TMAC deduced are strictly smaller than 1 excluding a complete diffuse reflection on the fused silica. The accommodation coefficient for Helium is significantly greater than the other gas coefficients.
- Table 1 shows a good agreement of the present values with other authors experimental results if considering that the geometry of [3], [6], [7] was not circular, that the surface materials were generally not exactly the same (generally silica and silicon are both involved for a part in the channel shape), and that finally the pressure is generally not the same; moreover, certain authors derived the TMAC from a first order treatment.
- In order to study the detailed influence of geometry or pressure ratio on the TMAC more systematic experiments would be needed, even if in our experiments the value obtained for \mathcal{P} with the Nitrogen and Argon seems to give results a little lower than other \mathcal{P} values.

CONCLUSIONS

This work contributes to clarify the validity domains of slip regime modelling using first or second order boundary conditions. For the gases considered in the 0.003 – 0.3 Kn range, in tube geometry, the second order fitting seems the most convenient. The TMAC determination leads to conclude that the He , Ar , and N_2 molecules are not reflected on silica surface following a full diffuse reflection. The Helium TMAC appears significantly greater than those of two other gases. To conclude on influence of inlet/outlet pressure ratio (or of geometry) on the accommodation process (for a same Knudsen number) would need more systematic experiments.

ACKNOWLEDGEMENTS

The authors are grateful to the CNRS (National Center of Scientific Research - project number MI2F03-45), the Conseil Régional Provence Alpes Côtes d’Azur and the SERES company for their financial support.

REFERENCES

1. PONG, K., HO, C., LIU, J., AND TAI, Y., *In Application of Microfabrication to fluid Mechanics ASME*, **197**, 51–56; 1994.
2. HARLEY, J., HUANG, Y., BAU, H., AND ZEMEL, J., *Journal of Fluid Mechanics*, **284**, 257–274, 1995.
3. ARKILIK, E.B., SCHMIDT, M.A., AND BREUER, K.S., *Journal of Microelectromechanical systems*, **6**, No. 2, 167–178 (1997).
4. ARKILIK, E.B., BREUER, K. AND SCHMIDT, M., *Journal of Fluid Mechanics*, **437**, 29–43, (2001).
5. ZOHAR, Y., LEE, S.Y.K., LEE, W.Y., JIANG, L. AND TONG, P., *Journal of FluidMechanics*, **472**, 125–151, 2002.
6. COLIN, S., LALONDE, P., AND CAEN, R., *Heat Transfer Eng.*, **25**, No. 3, 23–30, 2004.
7. MAURER, J., TABELIN, P., JOSEPH, P., AND WILLAIME, H., *Physic of fluid*, **15**, 2613–2621, 2003.
8. DONG, W., University of California Report No.UCRL-3353, 1956.
9. PORODNOV, B. T., SUETIN, P.E., BORISOV, S.F., AND AKINSHIN V.D., *Journal of Fluid Mechanics*, **64**, 417–437, 1974.
10. TISON, S.A., *Vacuum*, **44**, 1171–1175, 1993.
11. LALONDE, P., *Etude expérimentale d’écoulements gazeux dans les microsystèmes et fluides*, Ph. D thesis, Institut National des Sciences Appliquées, Toulouse, France, 2001.
12. SAXENA, S.C., AND R.K., JOSHI, Data series on material properties, Thermal Accomodation and Adsorption Coefficients of gases, **II.1**, 1981.
13. EWART, T., PERRIER, P., GRAUR, I., AND MÉOLANS, J.G., Experiments in fluids, online publication, 2006
14. KARNIADAKIS G.E., AND BESKOK A., *Microflows: fundamentals and simulation*, Springer, Berlin, New York, 2002.
15. CHAPMAN, S., AND COWLING, T.G., *The mathematical theory of non-uniform gases, third edition*, University Press, Cambridge, 1970.
16. BIRD, G.A., *Molecular gas dynamics and the direct simulation of gas flows*, Oxford University Press, New York, 1994.
17. GRAUR, I., MÉOLANS, J.G. AND ZEITOUN, D., *Microfluidics and Nanofluidics*, **2**, 64–77, 2006.